

Received Date : 22-Jan-2016

Revised Date : 31-Mar-2016

Accepted Date : 18-Jun-2016

Article type : Research Article

Design, synthesis, biological evaluation, NMR and DFT studies of structurally-simplified trimethoxy benzamides as P-glycoprotein selective inhibitors: the role of molecular flatness

*Angela Stefanachi^{‡1}, Giuseppe Felice Mangiatordi^{‡1}, Piero Tardia[‡], Domenico Alberga[§],
Francesco Leonetti[‡], Mauro Niso[‡], Nicola Antonio Colabufo[‡], Carlo Adamo[§], Orazio
Nicolotti^{‡*} and Saverio Cellamare^{‡*}*

[‡] Dipartimento di Farmacia – Scienze del Farmaco, Università di Bari Aldo Moro, Via Orabona 4, 70125, Bari, Italy.

[§] Dipartimento di Fisica, Università di Bari Aldo Moro, INFN & TIRES, Via Amendola 173, 70126 Bari, Italy

This article has been accepted for publication and undergone full peer review but has not been through the copyediting, typesetting, pagination and proofreading process, which may lead to differences between this version and the Version of Record. Please cite this article as doi: 10.1111/cbdd.12811

This article is protected by copyright. All rights reserved.

§ PSL Research University, Chimie ParisTech-CNRS, Institut de Recherche de Chimie Paris, Paris, France and Institut Universitaire de France, 103 Bd Saint-Michel, F-75005 Paris, France

¹ these authors contributed equally to this study

Abstract

In a recent investigation carried out on a panel of trimethoxybenzanilides, we showed that the formation of an intramolecular hydrogen bond is a key element for tuning P-gp inhibitory activity. In the present study, we designed new structurally-simplified trimethoxy benzamides (**5-17**, Table 1) with the aim to uncover the minimal molecular requirements needed for P-gp inhibition. The new prepared smaller-sized compounds exhibited IC₅₀ in the low micromolar range. The combined use of NMR and DFT studies suggested that molecular flatness is causatively related to the P-gp inhibition. Our results clearly pointed out that concerted theoretical and experimental approaches herein presented might be very helpful in addressing the design of structurally-simplified and highly efficient compounds biasing P-gp protein.

1. Introduction

It is widely acknowledged that molecular size, basicity and lipophilicity are determinant molecular properties to obtain potent and selective P-gp ligands.^{1,2} Less attention has instead been paid to other molecular features, such as the occurrence of intramolecular hydrogen bonds (IMHBs) and, more importantly, the propensity to result ring planar conformations. As well known, five- to eight-membered ring systems, and primarily the six-membered motifs, can benefit of π -delocalization. In this respect, an important effect of IMHB is that of increasing the lipophilic content since the formation of planar ring conformations reduces the level of exposure of polar groups. Of course, the conformation-dependent gain of

lipophilicity is relevant also in terms of membrane permeability.^{3,4} This issue has been the focus of recent important studies in medicinal chemistry.^{5,6}

ABCB1 (also named P-glicoprotein, P-gp or MDR1) and ABCC1 (Multidrug Resistance Protein 1 or MRP1) are efflux pumps members of the ATP binding cassette (ABC) transporters superfamily playing a crucial role in the active transport across plasma membrane of metabolites and detoxification of xenobiotics and drugs in numerous human tissues (such as blood-brain barrier, intestinal barrier and blood-cerebrospinal fluid barrier).⁷⁻⁹

The protective role of the ABC transporters is enhanced by the low substrate specificity that allows the active efflux of numerous structurally unrelated compounds. Chemotherapeutic pressure induces overexpression of these transporters in a wide range of cancer cells (breast cancer, colon cancer, leukemia), which reduces sensitivity to multiple anticancer agents (Multidrug Resistance, MDR).¹⁰⁻¹²

P-gp is the best-characterized member of the ABC family and evidences collected suggest that the protein is able to catch its substrates from the inner membrane leaflet and release them to either the extracellular medium or the outer membrane leaflet.¹³ Furthermore, the recently solved X-ray crystal structure of *Caenorhabditis elegans* P-gp showed the presence of an opening, easily accessible from the inner membrane bilayer, thus suggesting that drugs can enter the binding pocket from the plasma membrane.¹⁴ Consequently, it is easy to postulate that high lipophilicity is a key feature for high P-gp inhibitory activity. This is also supported by the linear correlation between this physicochemical property and the inhibitory activity found for several molecular scaffolds.^{15,16}

In a recent work carried out on a series of trimethoxybenzanilides, we reported that the establishment of an IMHB allows the fine-tuning of the P-gp inhibitory activity.¹⁷ This was likely due to the increase of the conformation-dependent lipophilicity that enabled to reach sub-micromolar IC_{50} values in terms of P-gp inhibitory activity. Interestingly, quantum

mechanics calculations and molecular dynamics simulation studies performed in the same previous work demonstrated that the IMHB was able to hold the most active compounds in a flat conformation and envisaged a certain trend between the strength of the HB and the P-gp inhibitory activity (1-4 Figure 1).

These intriguing results prompted us to prepare a new set of structurally-simplified trimethoxybenzanilides, designed with two aims: a) elucidating the impact of the IMHB at conformational level and its effects on the P-gp inhibitory activity; b) identifying the minimal molecular requirements needed to gain P-gp modulation. Thus, we designed and synthesized a set of trimethoxybenzanilides whose general scaffold was obtained by structural simplification of the previously reported compounds, a strategy widely applied in drug design to shorten synthetic routes and to reduce costs while keeping a certain biological activity.¹⁸⁻²⁰

Indeed, designing potent smaller-sized ligands is of utmost importance in medicinal chemistry to better elucidate, at molecular level, the nature of the driving forces behind the experimentally observed interactions and to minimize ADME attrition in late stage development.²¹ Herein, the molecular scaffold is simply made of a trimethoxybenzoyl moiety bound to an aniline ring (see Table 1). As far as the trimethoxybenzoyl moiety is concerned, all the possible regioisomers were designed and prepared to unveil the role of the ortho methoxy substituent in determining high P-gp inhibition and its importance in the formation of a stable IMBH (hereafter referred to as IMBH₁). On the other side, the aniline ring was decorated by using two different substituents that are a methoxy group and a bromine atom. The rationale behind this strategy of molecular design was that the ortho methoxy group (position R¹ of the aniline ring, see Scheme 1) might favor the occurrence of a second IMHB (hereafter referred to as IMHB₂) while the bromine atom would support the lipophilicity content. Satisfactorily, this approach allowed obtaining ligands with P-gp inhibitory activity

in the low micromolar range despite a lower molecular weight compared to previous studies.^{17,22,23} At the best of our knowledge, levels of P-gp inhibitory activity as good as those herein presented have never been observed so far for equally sized compounds. Finally, the results obtained employing Density Functional Theory (DFT) and NMR unequivocally suggest that molecular flatness could be a key property to enhance P-gp inhibition.

2. Chemistry

The synthesis of our derivatives **5-17** was accomplished very easily by a condensation between the corresponding acid, activated with thionyl chloride, and the aniline (Scheme 1).

The synthesis of compounds **5**,²⁴ **6**,²⁵ **9**,²⁶ **10**,²⁷ and **13**²⁸ was already described and their reported physical-chemical properties were coincident with that observed by us.

3. Results and discussion

3.1 Biochemical and lipophilicity studies

P-gp and MRP1 modulating activities of tested compounds were determined by fluorescence measurements, using calcein-AM fluorescent probes, in MDCK-MDR1 and MDCK-MRP1 cell lines.²⁹ These cells overexpress only P-gp or MRP1 transporters and, thus, the observed biological effects can be ascribed to the specific inhibition of these pumps. Calcein-AM is a lipophilic substrate of both P-gp and MRP1, able to cross the cell membrane. Inside the cell compartment, it is hydrolyzed by endogenous cytoplasmic esterases, yielding highly fluorescent calcein. The hydrolyzed compound is not a P-gp or MRP1 substrate, and it cannot cross the cell membrane via passive diffusion because it is too hydrophilic. Thus, a rapid increase in the fluorescence of cytoplasmic calcein can be monitored. P-gp and MRP1 transporters, expressed in the cell membrane, rapidly efflux the calcein-AM before its

entrance into the cytosol, giving a reduction of the fluorescent signal due to a decrease in the accumulation of calcein. Evaluation of P-gp or MRP1 activity in the presence of pump inhibitors can be performed in a competitive manner. Compounds that block P-gp and MRP1 pumps inhibit calcein-AM efflux, increasing intracellular accumulation of fluorescent calcein. Values of IC_{50} for calcein-AM uptake (Table 1) were determined by measuring relative fluorescence values obtained after 30 min of incubation at 37 °C. Verapamil and MC18³⁰ were used as reference compounds for MRP1 and P-gp inhibition, respectively. The accuracy and reproducibility of the estimated IC_{50} values are in accordance with the most recent guidelines.³¹ We have recently reported¹⁷ that there is a good relationship between the lipophilicity and the P-gp inhibitory activity of trimethoxybenzanilides. Actually, such a trend can be appreciated by measuring the value of $\log k'$ (the interested reader is referred to the “Experimental section” for details), an experimental lipophilicity index determined by HPLC using a reversed stationary phase in isocratic conditions. Building on this evidence, we have measured $\log k'$ values for the herein presented new set of structurally-simplified compounds. Inhibition data of P-gp and MRP1, lipophilicity measures and the ¹H NMR chemical shifts of the amidic proton (δ_{NH}) for all the investigated derivatives **5-17** are reported in Table 2. As shown in **Scheme 1**, all the investigated compounds are characterized by a common molecular scaffold consisting of an aniline and a trimethoxybenzoyl ring, respectively, joined through an amide bond. Importantly, a good activity is obtained (see for instance compounds **10**, **14** and **17**) despite the performed structural simplification of compounds (i.e., **1**, **2**, **3** and **4**), already discussed in our recently published work. Notably, such structural changes did not affect the high selectivity towards P-gp with respect to MRP1. Building on these observations, we attempted to identify the minimal molecular requirements needed for both efficient and selective P-gp modulation. In this respect, data reported in Table 1 enclose a wealth of information and enable us to draw important clues. First and

foremost, the majority of the compounds whose NMR data indicated the presence of IMHB₁ show both higher activity and lipophilicity with respect to regioisomers lacking of IMHB₁. For instance, this becomes clear by comparing **5** (IC₅₀ = 70.7 μM) with **6** (IC₅₀ = 21.9 μM) or, alternatively, **9** (IC₅₀ = 27.0 μM) with **10** (IC₅₀ = 9.3 μM). We also noticed that, despite the presence of a methoxy group in position R² (potentially IMHB acceptor from the amidic nitrogen atom), appreciable increases of lipophilicity and activity are not observed in case of 2,4,6-trimethoxy regioisomers with respect to the corresponding 3,4,5-trimethoxy ones. To this end, the interested reader can compare **8** (log k' = -0.16, IC₅₀ >100 μM), **12** (log k' = 0.16, IC₅₀ = 76.2 μM) and **16** (log k' = 0.13, IC₅₀ = 47.6 μM) with **5** (log k' = 0.09, IC₅₀ = 70.7 μM), **9** (log k' = 0.52, IC₅₀ = 27 μM) and **13** (log k' = 0.15, IC₅₀ = 26.2 μM). Furthermore, comparing experimental data of **14** (log k' = 0.51, IC₅₀ = 3.52 μM) and **17** (log k' = 0.87, IC₅₀ = 1.54 μM) with those of **6** (log k' = 0.26, IC₅₀ = 21.9 μM) and **10** (log k' = 0.65, IC₅₀ = 9.3 μM) respectively, it is evident that the presence of a methoxy group in position R¹ is responsible for both higher activity and lipophilicity. In particular, a close look at the δNH data (see Table 2) would suggest the likely formation of IMHB₂, whose main effect, at molecular level, would be that of favoring the occurrence of flat tetracyclic-like conformations. Surprisingly, 2,3,4-trimethoxy regioisomers, namely compounds **7** (IC₅₀ >100 μM) and **15** (IC₅₀ = 30.4 μM), do not display higher activities with respect to the corresponding 3,4,5-trimethoxy regioisomers, namely compounds **5** (IC₅₀ = 70.7 μM) and **13** (IC₅₀ = 26.2 μM). The only exception is represented by compound **11**, whose activity (IC₅₀ = 19.4 μM) is slightly higher than the corresponding 3,4,5-trimethoxy regioisomer, namely compound **9** (IC₅₀ = 27 μM). This is observed despite their ability to establish IMHB₁, as denoted by an increase of lipophilicity and of δNH (see Table 2). Such unexpected behavior of 2,3,4-trimethoxy regioisomers is also supported by their ability to drop down the linear relationship obtained when plotting log k' vs pIC₅₀. The removal of regioisomers **7**, **11** and

15 has the effect of improving correlation (from $r^2 = 0.563$ to $r^2 = 0.797$, see Figure 2). Next, the obtained data clearly indicate that the bromine atom at the para position of the aniline ring strongly increases both lipophilicity, according to its tabulated positive Hansch-Fujita π substituent constant,³² and P-gp activity, as evident by comparing compounds **9** ($\log k' = 0.52$, $IC_{50} = 27 \mu\text{M}$) with **5** ($\log k' = 0.09$, $IC_{50} = 70.7 \mu\text{M}$); **10** ($\log k' = 0.65$, $IC_{50} = 9.3 \mu\text{M}$) with **6** ($\log k' = 0.26$, $IC_{50} = 21.9 \mu\text{M}$); **11** ($\log k' = 0.75$, $IC_{50} = 19.4 \mu\text{M}$) with **7** ($\log k' = 0.35$, $IC_{50} > 100 \mu\text{M}$); **12** ($\log k' = 0.16$, $IC_{50} = 76.2 \mu\text{M}$) with **8** ($\log k' = -0.16$, $IC_{50} > 100 \mu\text{M}$) and finally **17** ($\log k' = 0.87$, $IC_{50} = 1.54 \mu\text{M}$) with **14** ($\log k' = 0.51$, $IC_{50} = 3.52 \mu\text{M}$). In summary, the above-discussed data unequivocally indicate some specific structural features for P-gp inhibition: 1) methoxy groups in positions R^2 , R^4 and R^5 , 2) bromine in position R , 3) a methoxy substituent in position R^1 . The sole compound fulfilling all these molecular requisites is the **17**, which thus, not surprisingly, shows the highest activity ($IC_{50} = 1.54 \mu\text{M}$) in the panel of the tested derivatives. Finally, although a good correlation between lipophilicity and activity was confirmed, three compounds were provided with IC_{50} values not complying the experimental lipophilicity data. Taken together these observations prompted us to seek further and more convincing explanations affecting the P-gp inhibitory activity.

3.2 H-NMR

Although new methods based on physicochemical parameters such as $\log P$ have been proposed to evaluate the presence of IMHB,³³ NMR spectroscopy still represents the most useful and accurate technique. In order to demonstrate the presence of IMHB, $\Delta\delta$ chemical shift for the amide NH was evaluated and 2D-NOESY experiments were performed.

Amide proton hydrogen bonded generally present higher δ chemical shift and it is reasonable to accept the same trend for amide NH intramolecular hydrogen bonded. Consequently, the

Accepted Article
difference of $^1\text{H-NMR}$ chemical shift ($\Delta\delta$) between NH of isomers differing for the ability of forming IMHB (i.e. 3,4,5 trimethoxy regioisomers) represents a feasible tool for obtaining evidence of this interaction. Thus the NH $^1\text{H-NMR}$ chemical shifts were measured and the $\Delta\delta$ were evaluated.

As expected, the $\Delta\delta$ observed for compounds bearing the 2-methoxy group on the benzoyl moiety are generally positive, clearly indicating the IMHB₁ with NH (Tables 2a and 2b). Interestingly, despite the presence of two methoxy groups on position 2 and 6, compounds **8**, **12** and **16** show negative $\Delta\delta$. It is reasonable to accept that the steric clash and the electrostatic repulsion between the carbonyl group and the 6-methoxy group force the amide linker and the aromatic ring in different planes disrupting the proximity required for the IMHB₁, as confirmed by DFT analysis.

Furthermore, compounds **13-17** present a 2-methoxy group on the aniline moiety matching the proximity required for establishing IMHB₂. $\Delta\delta$ was evaluated comparing analogs differing for the presence of the methoxy group on the aniline ring ($\Delta\delta'$). The $\Delta\delta'$ observed are positive in all cases, indicating the formation of the second IMHB (Figure 3b).

In order to confirm the results obtained from the evaluation of $\Delta\delta$ and $\Delta\delta'$, 2D-NOESY assessments on **9**, **10** and **17** as model compounds were performed. The hydrogen bonds freeze the molecular conformation and force the methoxy groups to lie in proximity to the amidic proton. Consequently, we focused on the interaction between the amide NH and both the ortho methoxy groups on the aniline and benzoyl moieties. Compound **9** does not present the features required for the intramolecular hydrogen bonding. Thus, the coupling between the amidic proton (**H^a**, s, 8.01 ppm) and both the in ortho position protons (**H^b**, s, 7.02 ppm and **H^c**, m, 7.52 ppm) is detectable (Figure 3a).

As expected, the cross-peak relative to the interaction between the amide NH ($\mathbf{H}^{\mathbf{a}'}$, s, 9.86 ppm) and the ortho methoxy protons ($\mathbf{H}^{\mathbf{d}}$, s, 4.04 ppm) occurs in **10**, clearly indicating the presence of the IMHB. This assumption is also confirmed by the lack of interaction with the $\mathbf{H}^{\mathbf{b}'}$ proton (Figure 3b). Compound **17** presents both the methoxy groups in proximity to the amide linker. The NOE effect of the amidic proton ($\mathbf{H}^{\mathbf{a}''}$, s, 10.58 ppm) with the protons of the methoxy groups ($\mathbf{H}^{\mathbf{d}'}$, s, 4.06 ppm and $\mathbf{H}^{\mathbf{e}}$, s, 3.97 ppm) and the lack of interaction with $\mathbf{H}^{\mathbf{c}''}$ and $\mathbf{H}^{\mathbf{b}''}$ confirm both the establishment of the IMHB with the ortho methoxy group on the aniline moiety and the presence of the three-center hydrogen bond (Figure 3c).

3.3 DFT

Based on a DFT-based investigation, we recently provided a solid rationale for the different P-gp activities (at the submicromolar level) observed for compounds **1-4**.¹⁷ Notably, the strength of the IMHB occurring in such compounds was proved to be a sensitive parameter for tuning, at molecular level, P-gp inhibition. Building on this evidence, we extended such approach to all the compounds herein investigated.

Preliminary studies on the optimized geometries

As a first step, we conducted an in-depth analysis of the obtained DFT optimized structures (see Figure 4).

As expected, one IMHB can be detected in compounds **6, 7, 8, 10, 11, 12** and **13** while the presence of methoxy substituent in position \mathbf{R}^1 (see scheme **1**) allows the formation of a second IMHB in compounds **14, 15, 16** and **17**. The reliability of the obtained DFT geometries is supported by the high correlation observed between the ^1H NMR chemical shift

of the amidic proton and the distance computed from the proton to the nitrogen atom ($r^2 = 0.873$, see Figure 5).

As shown in Figure 4, all the computed minima disclose an almost planar conformation, except for the trimethoxy phenyl moiety, whose coplanarity with respect to the remaining molecule depends on the presence of an IMHB involving such moiety and the amidine group. However, the picture emerged from this preliminary investigation suggests that, albeit necessary, the presence of one sole IMHB could not be a sufficient requisite to constrain flat molecular conformations. Indeed, it is certainly true that the computed minima for compounds where an IMHB cannot be established (**5** and **9**) prefer other than planar structural poses. Nevertheless, the computed minima of **8**, **12**, and **16** were far from flatness although an IMHB could be envisaged for the presence of a methoxy substituent at the ortho position. However, in this case, the second methoxy substituent at the other ortho position (2,4,6 trimethoxy regioisomers) would prevent hypothetical planar rearrangement to avoid the likely repulsive interaction between the amidic oxygen atom and the methoxy oxygen atom at position R⁶ (see lateral views in Figure 4). Importantly, slightly not-planar minima are obtained optimizing all the 2,3,4 trimethoxy regioisomers, despite the presence of an IMHB, as indicated also by the above-discussed lipophilicity and δNH values (see Table 2). Such geometries give a glimpse of a possible rational explanation of the unaccountably lower values of activity observed for all the 2,3,4 trimethoxy regioisomers with respect to the 2,4,5 trimethoxy regioisomers. It is indeed worthy to mention that molecular flatness was hypothesized to be a key requisite for obtaining good P-gp inhibitory³⁴ as observed for **6**, **10**, **17**, and **14** whose energetically favored conformations are planar.

Geometrical analysis

In order to assess in more detail the putative relationship between molecular flatness and P-gp response, we performed an in-depth analysis of the optimized structures. As shown in Figure 6, the molecular flatness of the tested derivatives could be evaluated through different dihedral angles:

- φ , measuring the rotation around the bond established between the amidic carbon atom and the benzoic ring;
- ψ , measuring the rotation around the amidic bond;
- ω , measuring the rotation around the bond engaged between the nitrogen atom and the aniline ring. In other words, we assume that a structure can be considered totally planar if φ , ψ and ω are at the same time equal to 180° . This held certainly true if we limit our definition to the molecular scaffold irrespective of all the substituents decorating the two aromatic rings.

Importantly, relationships between the IC_{50} values (μM) and the deviation from the total planarity ($180-|x|$ where x is the value of the dihedral resulting from the optimized geometry) computed for dihedrals φ , ψ and ω and considering all compounds having at least one IMHB can be found. Needless to say that compounds **7** and **8** were not considered since a specific value of IC_{50} is not available for such molecules (see Table 1).

Together with the dihedral angle φ , already proved to be important for tuning P-gp inhibition,¹⁷ a certain trend can be detected also for dihedrals ψ and ω (see Figure S1 in the Supporting Information). Notably, the closer is the dihedral angle to the complete flatness, the higher is the P-gp activity. This would suggest that behind the formation of IMHB₁ between the methoxy substituent in position R², a complete flatness of the entire molecular

scaffold is highly desirable to increase P-gp inhibitory activity. This is also consistent with the evidence that the presence of two IMHB, potentially able to constrain the molecular scaffold into a tetracyclic conformation, favours P-gp inhibition, as reported in Table 1. Beyond the performed geometrical analysis allowing us to speculate about a putative relationship between P-gp inhibitory activity and the DFT optimized geometries, we moved forward studying the energetic aspects that already proved to be crucial in our previous work. This was necessary to properly investigate the behaviour also of those compounds missing of IMHB and thus having a higher conformational freedom.

Energetic analysis

The picture emerged from the above discussed geometrical analysis indicates that the extended flatness to the entire molecular scaffold, shared by all the investigated derivatives, could be a key property to improve the P-gp inhibitory activity. As reported, all the investigated compounds preferred to stay in planar conformation during geometrical optimization, until a steric hindrance takes place. In other words, the optimized geometry is, in the end, that having the highest flatness. Building on this evidence, we estimated the energy required to reach a new stable although less planar conformation (local minimum) starting from the obtained minima. In doing that, we calculated the Potential Energy Profile (PEP) for the torsion around the dihedrals angle φ , ψ and ω , through relaxed SCAN calculations. Such profiles allowed us to derive an energetic parameter (E_p), computed following the equation (1):

$$E_p = \min_{i=\varphi,\psi,\omega} \{E_i^{bar}\} \quad (1)$$

Where E_i^{bar} corresponds to the energy barrier required reaching a local (less planar) minimum starting from the optimized geometry, as resulting from the PEP of the dihedral i torsion (see

Figure S2 in the supporting information for a three meaningful examples of the E_i^{bar} computation). Briefly, E_p indicates the minimum value of energy barrier required to move far away from point intercepting the highest flatness, displayed by the optimized structure, whatever dihedral (ϕ , ψ and ω) is considered. For each considered compound both E_p value and dihedral angle providing the lowest E_{bar} value are reported in Table S1 (see Supporting Information). Note that dihedral ψ returns always E_ψ^{bar} much higher than the others since it describes the torsion around a partial double bond. For instance, considering compound **6**, E_ϕ^{bar} was equal to the energy required to break the IMHB occurring between the trimethoxy moiety and the amide group. Such value was obviously higher with respect to that required reaching a new local minimum having a less-planar ω angle, thus we considered for compound **6** $E_p = E_\omega^{bar}$. Importantly, the relationship ($r^2 = 0.835$) between E_p and the IC50 values (μM) is shown in Figure 7. Note that herein all compounds for which a value of inhibitory activity is available were considered. Satisfactorily, a very good correlation was detected confirming the importance of flatness for P-gp activity. More importantly, such relationship comprised also compounds **11** and **15**, whose activities were not predictable on the basis of lipophilicity and NMR studies.

The robustness of the herein relationship was further challenged performing an intensive y-randomization analysis to avoid the risk of chance correlations.³⁵ In this respect, we performed 1 million of y-scrambling runs to assess that the reliability and goodness of the correlation shown in Figure 7. Satisfactorily, all the scrambled r^2 obtained values were far from that reported in Figure 7. For the sake of completeness, we reported the distribution of scrambled r^2 in Figure 8. Finally, the robustness of the found correlation is also supported by the computed r_p^2 value equal to 0.730, which largely exceeds the recommended threshold of

0.500^{36,37} (the interested reader is referred to the Experimental section for methodological details).

Conclusions

The present paper reports how the harmonized use of experimental and theoretical approaches can be helpful to address the design of small-sized and efficient molecules selectively inhibiting P-gp. Our effort to streamline the molecular structures of our recently published compounds¹⁷ allowed us to detect the essential requirements needed to gain P-gp modulation, being the obtained low micromolar activity never observed before for equally sized compounds. Furthermore, the results obtained from an in-depth DFT based investigation suggest a solid and causative relationship between the energy required reaching a local (less planar) minimum starting from an optimized geometry and the observed activity. We do believe that our achievements might constitute a feasible molecular strategy to address the design of new, potent and selective P-gp inhibitors.

Experimental section

High analytical grade chemicals and solvents were purchased from commercial suppliers. When necessary, solvents were dried by standard techniques and distilled. Thin layer chromatography (TLC) was performed on aluminum sheets precoated with silica gel 60 F254 (0.2 mm) (E. Merck). Chromatographic spots were visualized by UV light. Purification of crude compounds was carried out by flash column chromatography on silica gel 60 (Kieselgel 0.040–0.063 mm, E. Merck) or by preparative TLC on silica gel 60 F254 plates or crystallization. ¹H NMR spectra were recorded in DMSO-d₆ or CDCl₃ at 300 MHz on a Varian Mercury 300 instrument. Chemical shifts (δ scale) are reported in parts per million (ppm) relative to the central peak of the solvent. Coupling constant (J values) are given in

Accepted Article
hertz (Hz). Spin multiplicities are given as s (singlet), br s (broad singlet), d (doublet), t (triplet), dd (double doublet), dt (double triplet), or m (multiplet). LRMS (ESI) was performed with an electrospray interface ion trap mass spectrometer (1100 series LC/MSD trap system Agilent, Palo Alto, CA). In all cases, spectroscopic data are in agreement with known compounds and assigned structures. Combustion analyses were performed by Eurovector Euro EA 3000 analyzer (Milan, Italy) and gave satisfactory results (C, H, N within 0.4% of calculated values).

Chromatographic settings. Logk' values and purity determinations were carried out using a Zorbax 300SB-C18 4.6 x 250mm, with 5 µm size particles, built on a Waters double pump HPLC system in isocratic conditions. Injection volumes were 5 µL, flow rate was 1 mL/min, detection was performed with UV ($\lambda=230$ nm and 254 nm). Samples were prepared by dissolving 0.1 mg/mL of the solute in 10% (v/v) DMSO and 90% (v/v) methanol. Retention times (t_r) were measured at least from three separate injections, dead time (t_0) was the retention time of deuterated water. The mobile phase was filtered through a Nylon 66 membrane 0.45µm (Supelco, USA) before use. For each reference compound, the average retention time (t_r) of three consecutive injections of 5 µL of sample was used to calculate the log k' values ($\log k' = \log[(t_r - t_0)/t_0]$). The eluent consisted of three different mixtures of methanol and PBS buffer at pH 7.4: the first measurement was 80% (v/v) methanol and 20% (v/v) of buffer; 70% (v/v) methanol and 30% (v/v) of buffer; 60% (v/v) methanol and 40% (v/v) of buffer.

The synthesis of N-(4-Bromo-phenyl)-3,4,5-trimethoxy-benzamide **9** was already reported.²⁶

General procedure for the preparation of benzamides 5-17

The starting benzoic acid (0.75 mmol) was suspended under argon in thionyl chloride (1.0 mL) and stirred for 3h at room temperature. The unreacted excess of thionyl chloride was removed under nitrogen flow to afford the corresponding benzoyl chloride. The solid

obtained and the appropriate aniline (0.50 mmol) were dissolved in the minimum volume of THF dry and stirred at room temperature for 6h. The suspension obtained was filtered and the residue was purified by crystallization or column chromatography affording the desired product.

3,4,5-Trimethoxy-N-phenyl-benzamide 5²⁴

Purified by chromatography (hexane/ethyl acetate, 60:40). Yield:37 %; mp:141-143 °C; ¹H NMR (CDCl₃) δ: 3.90 (s, 6H), 3.93 (s, 3H), 7.07 (s, 2H), 7.16 (tt, *J*=1.2 , 7.8, 1H), 7.38 (t, *J*=7.8 Hz, 2H), 7.63 (dd, *J*=1.2 ,7.8 Hz, 2H), 7.72 (s, 1H); LRMS (ESI) *m/z*: = 287 [M-H]⁻.

2,4,5-Trimethoxy-N-phenyl-benzamide 6²⁵

Purified by chromatography (hexane/ethyl acetate, 60:40). Yield:43%; m.p.=119-121 °C; ¹H NMR CDCl₃ δ 3.93 (s, 3H), 3.96 (s, 3H), 4.05 (s, 3H), 6.57 (s, 1H), 7.14-7.08 (m,1H),7.30-7.41 (m, 2H), 7.67 (dd, *J*=1.1, 8.5 Hz 2H), 7.82 (s, 1H), 9.84 (s, 1H); LRMS (ESI) *m/z*: = 287[M-H]⁻.

2,3,4-Trimethoxy-N-phenyl-benzamide 7

Purified by chromatography (hexane/ethyl acetate, 70:30). Yield:53 %; m.p. =107-109 °C;¹H NMR CDCl₃ δ 3.91 (s, 3H), 3.93 (s, 3H), 4.06 (s, 3H), 6.85 (d, *J*=8.9 Hz, 1H), 7.09-7.15 (m,1H), 7.34-7.39(m, 2H), 7.68 (dd, *J*=0.96, 8.7 Hz, 2H), 7.99 (d, *J*= 8.9 Hz, 1H), 9.97 (s, 1H); LRMS (ESI) *m/z*: = 287 [M-H]⁻.

2,4,6-Trimethoxy-N-phenyl-benzamide 8

Purified by chromatography (hexane/ethyl acetate, 70:30).Yield:17 %; p.f.:155-157 °C; ¹H NMR (CDCl₃) δ: 3.82 (s, 6H), 3.84 (s, 3H), 6.14 (s, 2H), 7.1 (t. *J*=7.4 Hz,1H), 7.35-7.31 (m 2H), 7.49 (s, 1H), 7.64 (d, *J*=7.9 Hz, 2H), LRMS (ESI) *m/z* : = 287[M-H]⁻.

N-(4-Bromo-phenyl)-2,4,5-trimethoxy-benzamide 10²⁷

Purified by chromatography (hexane/ethyl acetate, 60:40).Yield: 15 %; mp:82-84 °C;¹H NMR (CDCl₃) δ: 3.92 (s, 3H), 3.96 (s, 3H), 4.05 (s, 3H), 6.56 (s, 1H), 7.45 (dd, *J*=1.9, 6.9 Hz, 2H),7.57 (dd, *J*=1.92 , 6.87, 2H), 7.79 (s, 1H), 9.86 (s, 1H); LRMS (ESI) *m/z*: = 367 [M-H]⁻.

N-(4-Bromo-phenyl)-2,3,4-trimethoxy-benzamide 11

Purified by chromatography (hexane/ethyl acetate, 70:30). Yield: 61%; mp:145-147 °C; ¹H NMR (CDCl₃) δ: 3.90 (s, 3H), 3.93 (s, 3H), 4.06 (s, 3H), 6.83 (d *J*=9.1 Hz, 1H), 7.46 (dd, *J*=2.2, 6.8 Hz, 2H), 7.58 (dd, *J*=2.2, 6.8 Hz, 2H), 7.97 (d, *J*=9.1 Hz, 1H), 10.00 (s, 1H); LRMS (ESI) *m/z*: = 367 [M-H]⁻.

N-(4-Bromo-phenyl)-2,4,6-trimethoxy-benzamide 12

Purified by chromatography (hexane/ethyl acetate, 70:30). Yield: 22 %; mp:218-220 °C; ¹H NMR CDCl₃ δ 3.82 (s, 6H), 3.84 (s, 3H), 6.14 (s, 2H), 7.43 (d. *J*=8.8, 2H), 7.52 (s, 1H).7,54 (d, *J*=8.79, 2H); LRMS (ESI) *m/z*: = 367 [M-H]⁻.

3,4,5-Trimethoxy-N-(2-methoxy-phenyl)-benzamide 13²⁸

Purified by chromatography (hexane/ethyl acetate, 60:40). Yield: 63%; mp:118-120°C; ¹H NMR CDCl₃ δ 3.90 (s, 3H), 3.92 (s, 3H), 3.94 (s, 6H), 6.92 (dd, *J*=1.7, 7.9 Hz, 1H), 7.12-6.99 (m, 4H), 8.43 (s, 1H), 8.47 (dd, *J*=1.7, 7.9 Hz, 1H); LRMS (ESI) *m/z*: [M-H]⁻ = 317.

2,4,5-Trimethoxy-N-(2-methoxy-phenyl)-benzamide 14

Purified by crystallization EtOH/Et₂O. Yield: 34%; mp:180-182; °C, ¹H NMR CDCl₃ δ 3.93 (s, 3H), 3.95 (s, 3H), 3.96 (s, 3H), 4.06 (s, 3H), 6.57 (s, 1H), 6.93 (dd, *J*=1.8, 7.6 Hz, 1H), 7.00-7.05 (m, 2H), 7.83 (s,1H), 8.63 (dd, *J*=1.8, 7.6 Hz, 1H), 10.62 (s, 1H); LRMS (ESI) *m/z*: = 317 [M-H]⁻.

2,3,4-Trimethoxy-N-(2-methoxy-phenyl)-benzamide 15 Purified by chromatography (hexane/ethyl acetate, 70:30). Yield: 63%; mp:118-120 °C; ¹H NMR (CDCl₃) δ: 3.91: (s, 3H), 3.93 (s, 3H), 3.96 (s, 3H), 4.09 (s, 3H), 6.82 (d, *J*=9.1 Hz, 1H), 6.92 (dd, *J*=1.5, 7.8 Hz, 1H), 7.00-7.08 (m, 2H), 8.03 (d, *J*=9.1 Hz, 1H), 8.62 (dd, *J*=1.9, 7.8 Hz, 1H), 10.72 (s, 1H); LRMS (ESI) *m/z*: = 317 [M-H]⁻.

2,4,6-Trimethoxy-N-(2-methoxy-phenyl)-benzamide 16

Purified by crystallization EtOH/Et₂O. Yield: 15% ; mp:168.5-170.5 °C; ¹H NMR (CDCl₃) δ 3.81 (s, 9H), 3.84 (s, 3H), 6.14 (s, 2H), 6.87 (dd, *J*=2.0; 7.6 Hz, 1H), 6.96-7.06 (m, 2H), 8.21 (s,1H), 8,63 (dd, *J*=2.0, 7.6 Hz, 1H). LRMS (ESI) *m/z*: = 317[M-H]⁻.

4-bromo-2-methoxy-N-(2,4,5-trimethoxyphenyl)benzamide 17

Purified by chromatography (hexane/ethyl acetate, 70:30). Yield:15 %; m.p.:168,5-170,5 °C; ¹H NMR (CDCl₃) δ: 3.94 (s, 3H), 3.96 (s, 3H), 3.98 (s, 3H), 4.07 (s, 3H), 6.56 (s, 1H), 7.03 (d, *J*=1.5 Hz, 1H), 7.14 (dd, *J*=1.5, 8.3 Hz, 1H), 7.81 (s,1H), 8.55 (d, *J*=8.3 Hz, 1H), 10.58 (s, 1H); LRMS (ESI) *m/z*: = 395 [M-H].

Biology

Materials. CulturePlate 96/wells plates was purchased from PerkinElmer Life and Analytical Sciences (Boston, MA, USA). Cell culture reagents were obtained from EuroClone (Milan, Italy). Calcein-AM, was obtained from Sigma-Aldrich (Milan, Italy).

Cell Culture. MDCK-MDR1 and MDCK-MRP1 cells was a gift of Prof. P. Borst, NKI-AVL Institute, Amsterdam, Nederland. MDCK-MDR1 and MDCK-MRP1 cells were grown in DMEM high glucose supplemented with 10% fetal bovine serum, 2 mM glutamine, 100 U/mL penicillin, 100 µg/mL streptomycin, in a humidified incubator at 37 °C with a 5 % CO₂ atmosphere.

Calcein-AM experiment. These experiments were carried out as described by Colabufo et al. with minor modifications.²⁹ Calcein-AM is a profluorescent probe and is a P-gp substrate.

In cells overexpressing P-gp or MRP1, Calcein-AM is not able to permeate cell membrane whereas when the efflux pump is not present or is inhibited, the probe enters living cells and is converted to fluorescent Calcein by intracellular esterases. Calcein is not able to diffuse through the membrane since it is hydrophilic and is not a P-gp or MRP1 substrate; thus, Calcein accumulates in cells when the pump is blocked. Therefore, the fluorescent signal is directly correlated to the amount of P-gp or MRP1 interaction. MDCK-MDR1 or MDCK-MRP1 cells (50,000 cells per well) were seeded into black CulturePlate 96/wells plate with 100 µL medium and allowed to become confluent overnight. 100 µL of test compounds were solubilized in culture medium and added to monolayers. 96/Wells plate was incubated at 37

°C for 30min. Calcein-AM was added in 100 μ L of Phosphate Buffered Saline (PBS) to yield a final concentration of 2.5 μ M and plate was incubated for 30 min. Each well was washed 3 times with ice cold PBS. Saline buffer was added to each well and the plate was read to Victor3 (PerkinElmer) at excitation and emission wavelengths of 485 nm and 535 nm, respectively. In these experimental conditions Calcein cell accumulation in the absence and in the presence of tested compounds was evaluated and fluorescence basal level was estimated by untreated cells. In treated wells the increase of fluorescence with respect to basal level was measured. IC₅₀ values were determined by fitting the fluorescence increase percentage versus log[dose].

Computational details

All DFT calculations were carried out using the Gaussian 09 package.³⁸ Geometry optimizations were performed at the B3LYP³⁹/6-311G(d,p) level of theory and in gas phase. Harmonic vibrational frequency analyses were applied in order to confirm the nature of the localized stationary states. Relaxed scan calculations were performed using the same level of theory and a step size equal to 10 degrees (i.e. total number of steps equal to 36 for each considered dihedral).

Model validation

The robustness of the found correlation was challenged by performing a randomization analysis. In order to assess the risk of chance correlation 1 million of y-scrambled models were generated and for each of them a value of r^2 was computed. Notably, the found correlation can be considered statistically significant if for all the randomized models a value of r^2 lower than that observed for the non-randomized model is detected. Furthermore we also computed the r_p^2 parameter³⁷ following the equation:

$$r_p^2 = r^2 * \sqrt{(r^2 - r_{SCR}^2)}$$

(2)

Where r^2 is the squared correlation coefficient of the non-randomized model and r_{SCR}^2 is the squared correlation coefficient averaged over all the randomized models. A value of r_p^2 higher than 0.5 ensures that the obtained correlation is not obtained by chance.³⁷

Acknowledgements

The authors thank the program FIRB (Futuro in Ricerca 2012, RBF12SJA8_003) and the Programma IDEA 2011. We acknowledge the CINECA awards no. HP10CWS1PD under the IS CRA initiative for the availability of high-performance computing resources and support.

Conflict of interest

The authors declare no conflict of interest

AUTHOR INFORMATION Corresponding Authors: phone, +39-080-5442551/+39-080-5442090; fax, +39-080-5442230; E-mails, orazio.nicolotti@uniba.it/saverio.cellamare@uniba.it.

Abbreviations: MDR, multidrug resistance; P-gp, P-glycoprotein; MRP1, human multidrug resistance associate-protein 1; intramolecular hydrogen bond, IMHB; Density Functional Theory DFT

Scheme captions

Scheme 1. Synthesis of compounds **5-17**.

Figure captions

Figure 1. Chemical structure and P-gp inhibitory activity of trimethoxy benzamides investigated in the previous study.

Figure 2. Relationships between P-gp inhibitory potency (pIC_{50}) of compounds listed in Table 1 and experimental $\log k'_{70\%MeOH}$ values.

Figure 3. a) 2D NOESY of compound **9**; b) 2D NOESY of compound **10**; c) 2D NOESY of compound **17**.

Figure 4. Structures of energy minima resulting from DFT optimization. All calculations were performed at the B3LYP/6-311G(d, p) level of theory. IMHBs are depicted as dotted lines. Computed distances between the hydrogen and the acceptor oxygen involves in all the detected IMHB₁ ($d_{1(O-H)}$) and IMHB₂ ($d_{2(O-H)}$) are reported in Å.

Figure 5. Relationship between the experimental 1H NMR chemical shift of the exchangeable NH proton and the computed H-N distance (Å) of the optimized DFT structures.

Figure 6. Sketch of the dihedral angles considered as representative of the molecular flatness in the investigated compounds.

Figure 7. Relationship between the IC_{50} values and E_p values computed according to the equation (1).

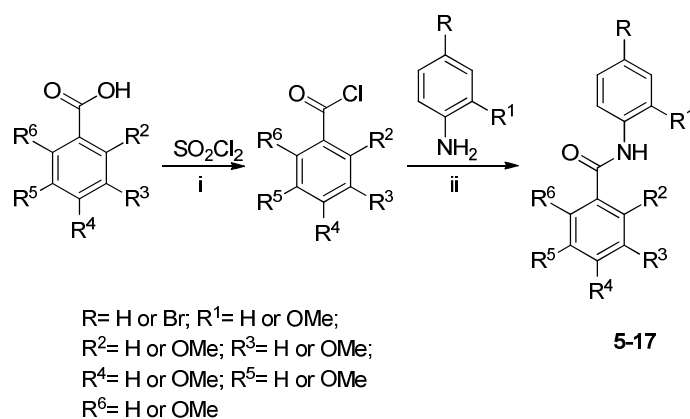
Figure 8. Histogram of r^2_{SCR} vs. number of randomized models over 1 million y-scrambling runs.

Table Captions

Table 1. Chemical structure, biological activity and experimental measures of lipophilicity of the compounds **5-17**.

Table 2. ^1H NMR chemical shifts of the amidic proton (δNH) of the considered compounds and a) its variation with respect to the corresponding 3,4,5, trimethoxy regioisomers ($\Delta\delta\text{NH}$); b) its variation with respect to the analog differing for the presence of the methoxy group on the aniline ring ($\Delta\delta'\text{NH}$).

Scheme 1



Reagents and conditions: i) neat Thionyl chloride 3h; reflux; ii) DRY THF, r. t., 6h.

Figure 1

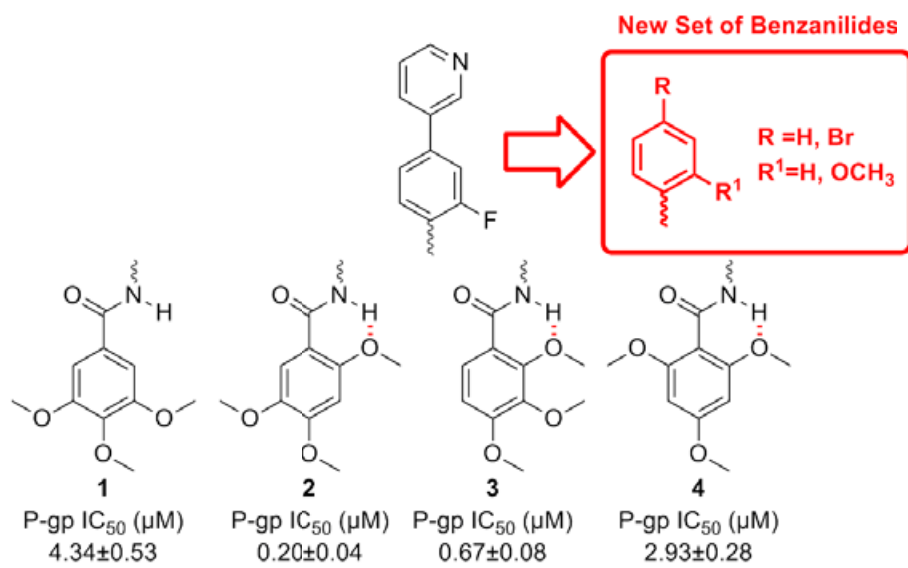
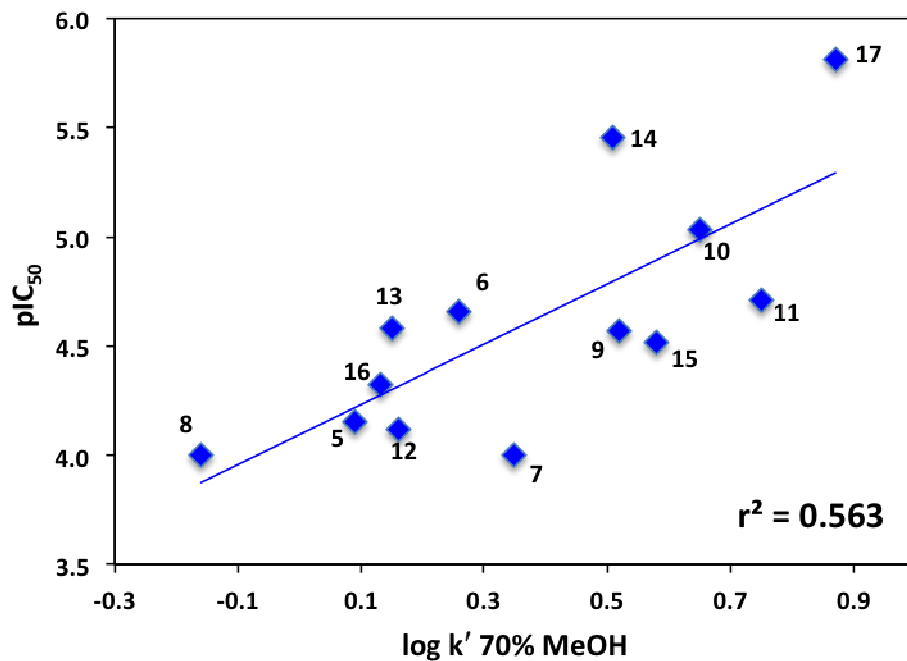


Figure 2

a)



b)

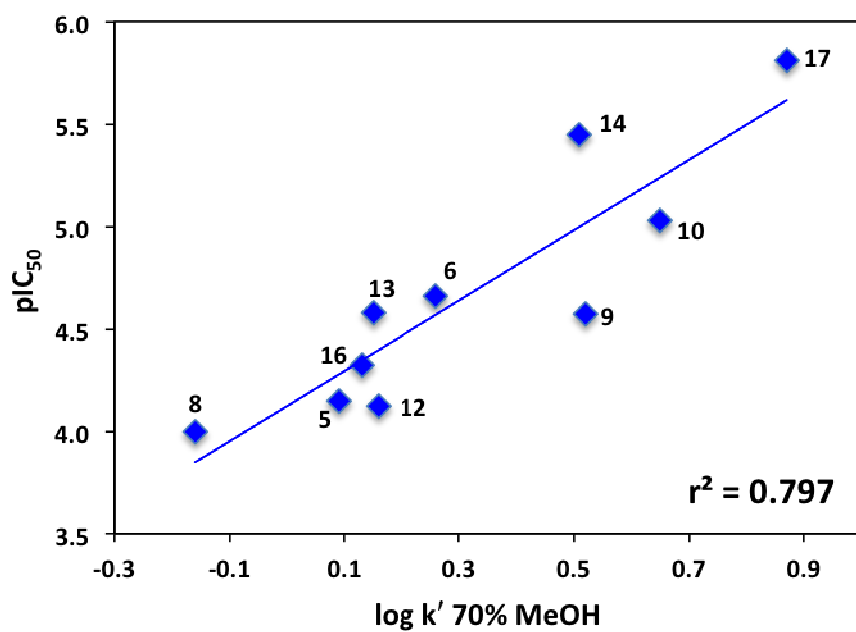
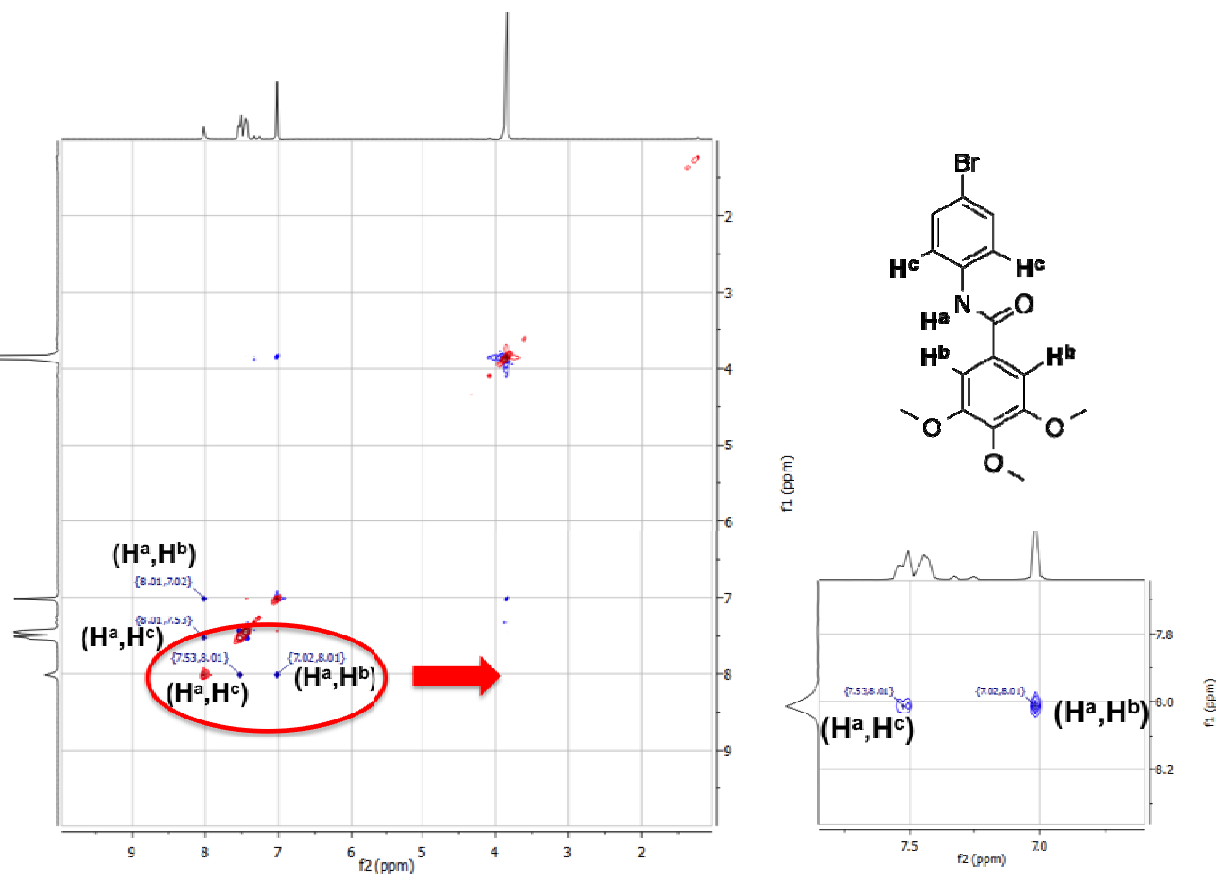


Figure 3

a)



b)

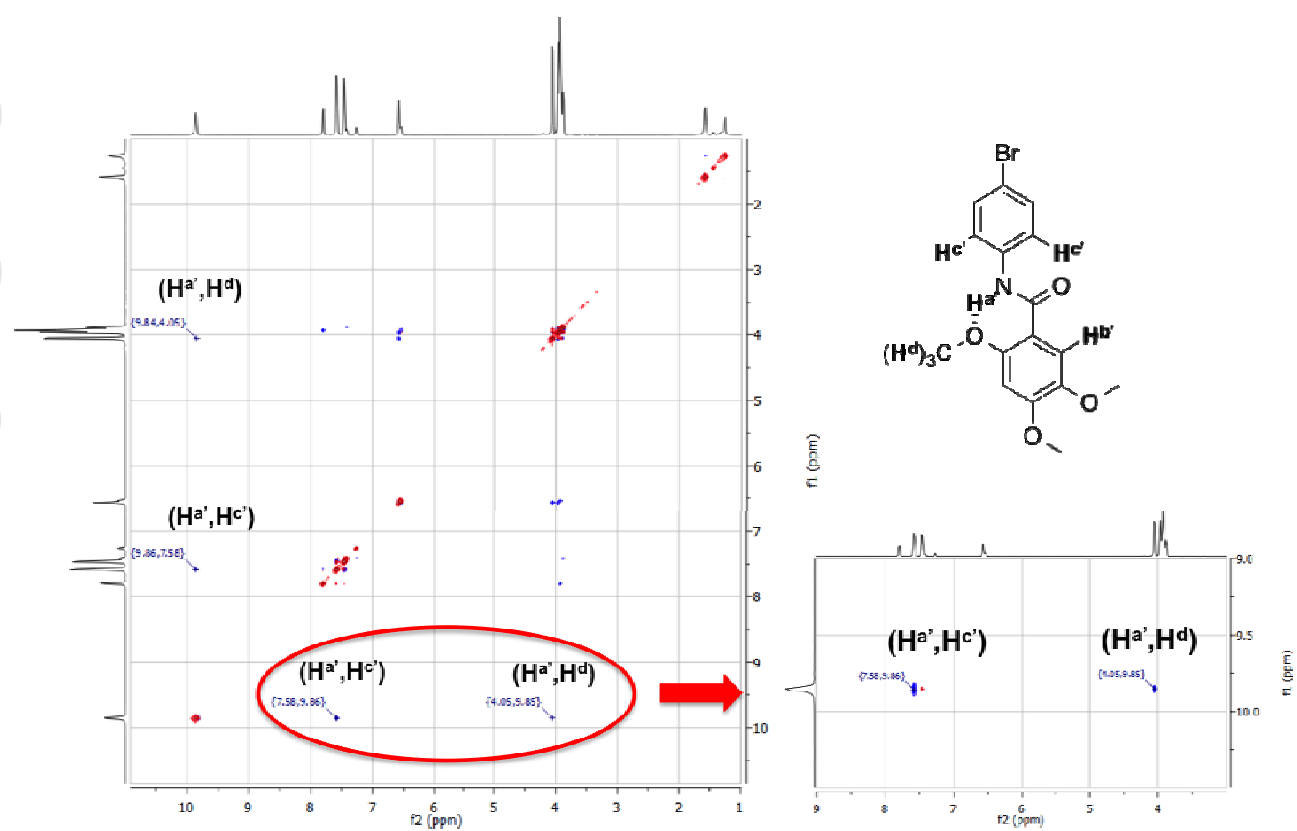


Figure 4

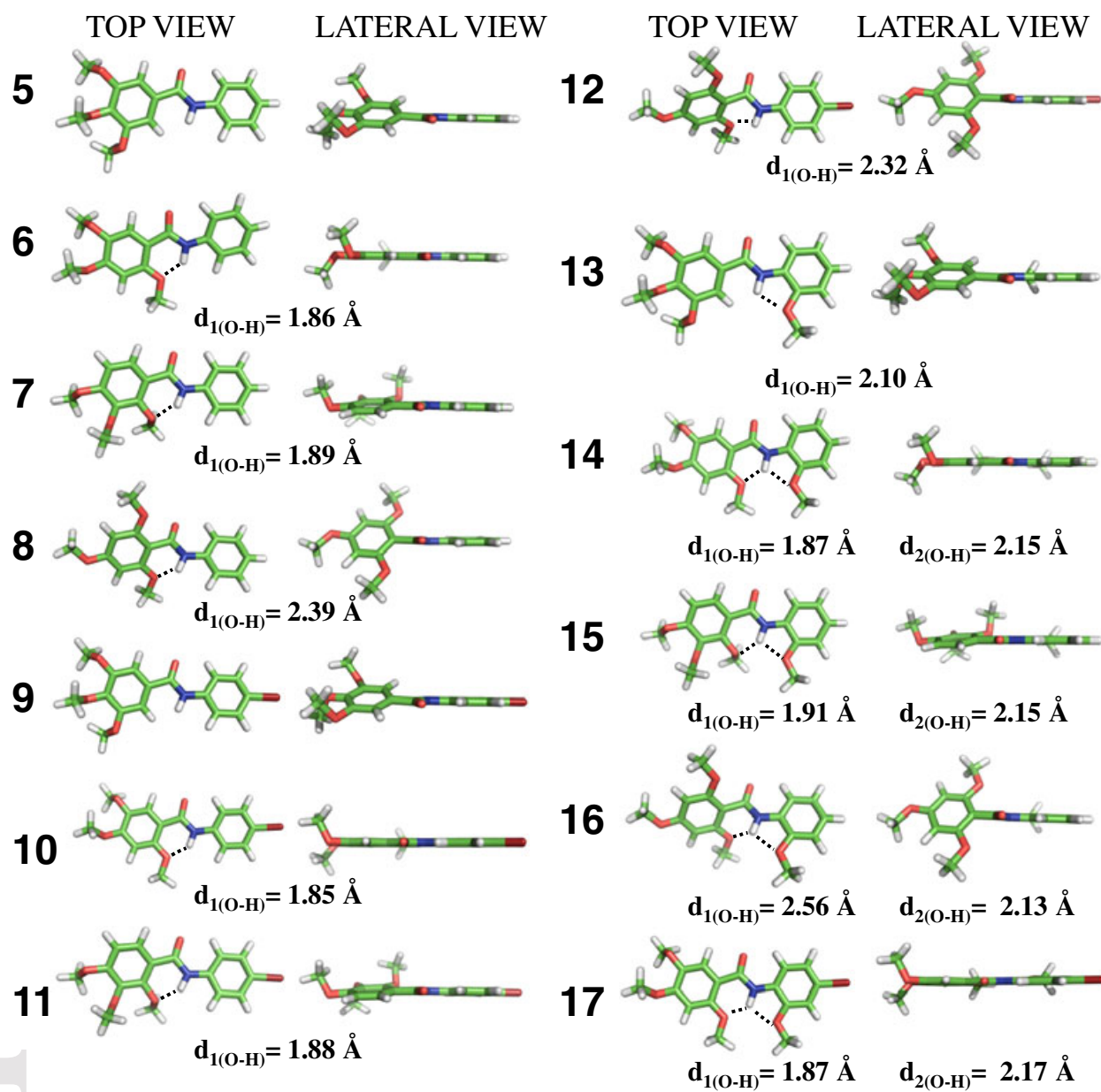


Figure 5

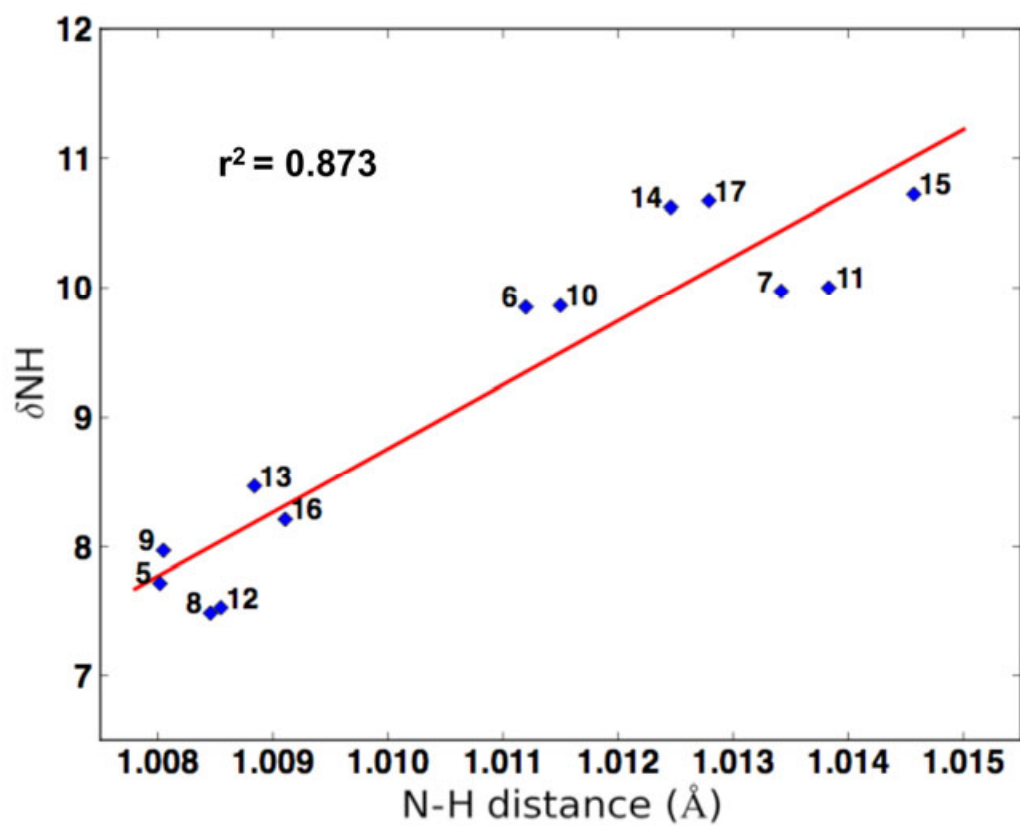


Figure 6

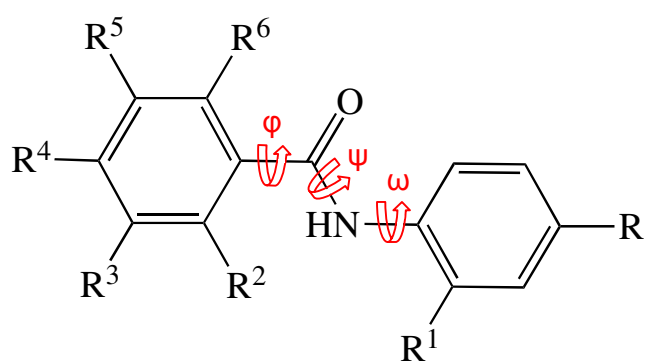


Figure 7

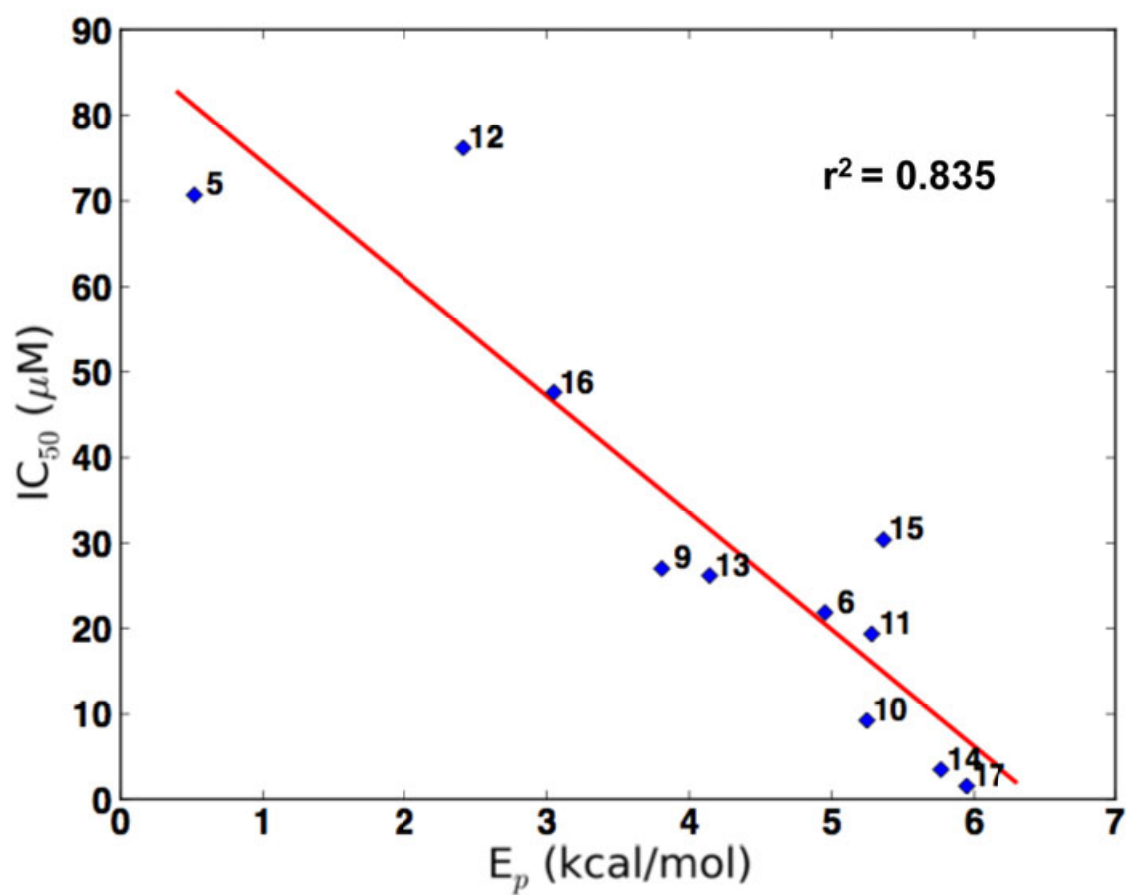


Figure 8

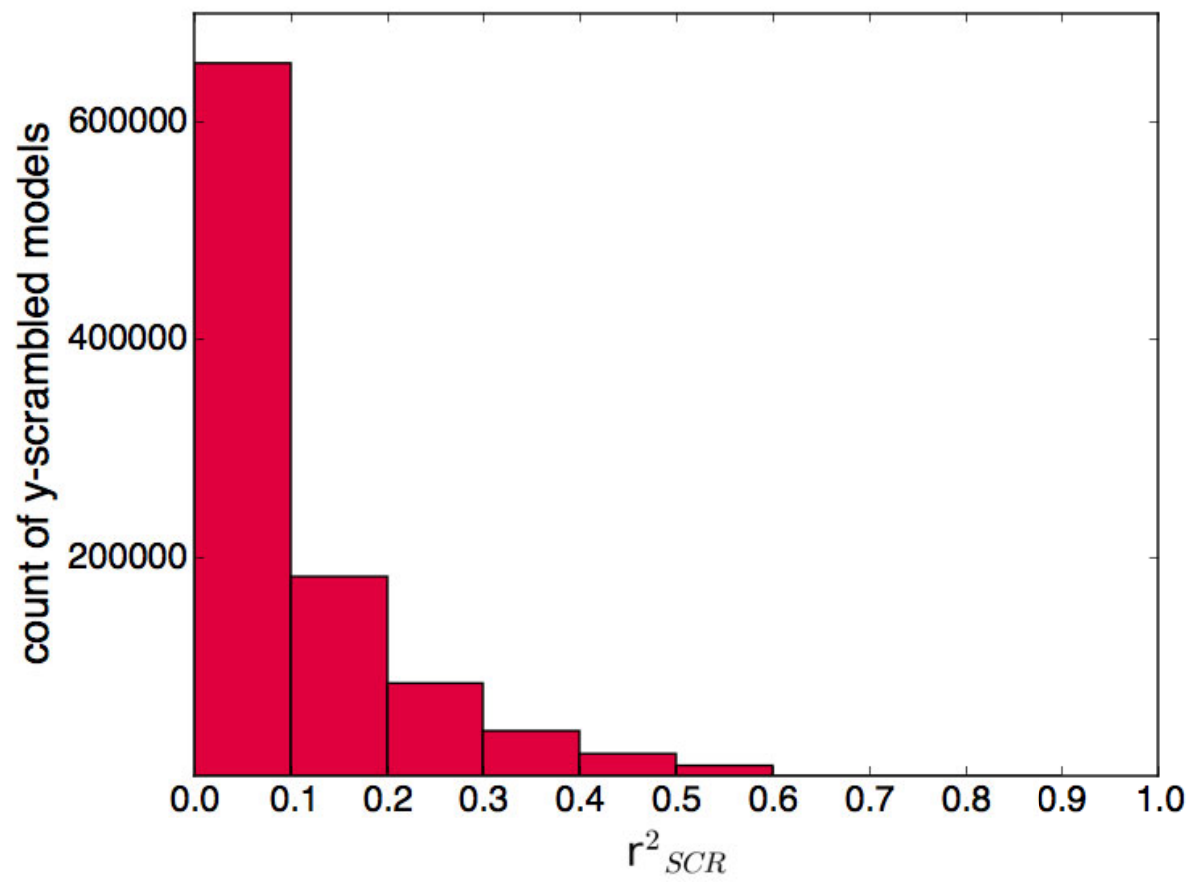
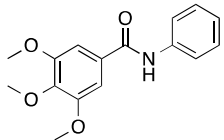
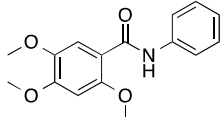
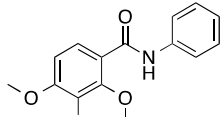
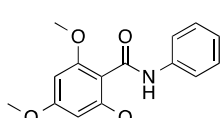
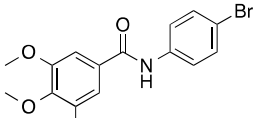
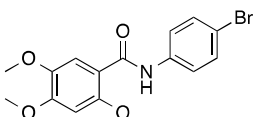
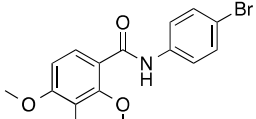
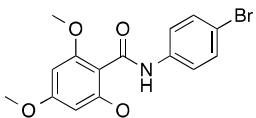
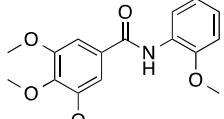
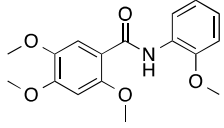
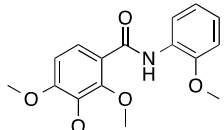
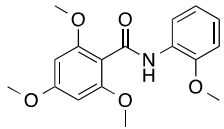
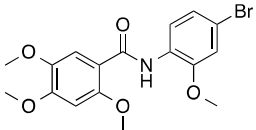


Table 1

Cpd	Structure	P-gp ^a	MRP1	log k ^b
5		70.7±9.01	>100	0.09
6		21.9±3.01	>100	0.26
7		>100	>100	0.35
8		>100	>100	-0.16
9		27±3.78	>100	0.52
10		9.27±1.29	>100	0.65
11		19.4±2.71	>100	0.75
12		76.2±10.6	>100	0.16
13		26.2±3.67	>100	0.15

14		3.52±0.49	>100	0.51
15		30.4±4.21	71.0	0.58
16		47.6±6.66	>100	0.13
17		1.54±0.21	>100	0.87
MC18 ^c		1.01±0.21		
Verapamil			3.53±0.43	

a) The IC₅₀ data (Calcein-AM assay), reported as μM ± SEM, are averaged over two independent experiments, sampled in triplicate; b) logarithm of the capacity factors measured by RP-chromatography using methanol/pH 7.4 phosphate buffer 70:30 as an eluent; c) reference compound³⁰

Table 2

a)

Cpd	Substitution pattern	δ NH (ppm)	$\Delta\delta$ NH (ppm)
5	3,4,5	7.72	
6	2,4,5	9.85	2.13
7	2,3,4	9.97	2.25
8	2,4,6	7.49	-0.23
9	3,4,5	7.97	
10	2,4,5	9.86	1.89
11	2,3,4	10.0	2.03
12	2,4,6	7.53	-0.44
13	3,4,5	8.47	
14	2,4,5	10.62	2.15
15	2,3,4	10.72	2.25
16	2,4,6	8.21	-0.26
17*	2,4,5	10.67	

b)

Cpd	δ NH (ppm)	$\Delta\delta'$ NH (ppm)
5	7.72	
13	8.47	0.75
6	9.85	
14	10.62	0.77
7	9.97	
15	10.72	0.75
8	7.49	
16	8.21	0.72
10	9.86	
17	10.67	0.81

* $\Delta\delta$ NH not reported (absence of the corresponding 3,4,5, regioisomer)

References

1. Broccatelli, F.; Carosati, E.; Neri, A.; Frosini, M.; Goracci, L.; Oprea, T. I.; Cruciani, G. *J. Med. Chem.* **2011**, *54*, 1740–1751.
2. Ueda, K.; Taguchi, Y.; Morishima, M. *Semin. Cancer Biol.* **1997**, *8*, 151–159.
3. Kuhn, B.; Mohr, P.; Stahl, M. *J. Med. Chem.* **2010**, *53*, 2601–2611.
4. Ettore, A.; D'Andrea, P.; Mauro, S.; Porcelloni, M.; Rossi, C.; Altamura, M.; Catalioto, R. M.; Giuliani, S.; Maggi, C. A.; Fattori, D. *Bioorg. Med. Chem. Lett.* **2011**, *21*, 1807–1809.
5. Over, B.; McCarren, P.; Artursson, P.; Foley, M.; Giordanetto, F.; Grönberg, G.; Hilgendorf, C.; Lee, M. D.; Matsson, P.; Muncipinto, G.; Pellisson, M.; Perry, M. W. D.; Svensson, R.; Duvall, J. R.; Kihlberg, J. *J. Med. Chem.* **2014**, *57*, 2746–2754.
6. Alex, A.; Millan, D. S.; Perez, M.; Wakenhut, F.; Whitlock, G. A. *MedChemComm* **2011**, *2*, 669–674.
7. Silva, R.; Vilas-Boas, V.; Carmo, H.; Dinis-Oliveira, R. J.; Carvalho, F.; de Lourdes Bastos, M.; Remião, F. *Pharmacol. Ther.* **2015**, *149*, 1–123.
8. Thiebaut, F.; Tsuruo, T.; Hamada, H.; Gottesman, M. M.; Pastan, I.; Willingham, M. *C. Proc. Natl. Acad. Sci. U. S. A.* **1987**, *84*, 7735–7738.
9. Croop, J. M.; Raymond, M.; Haber, D.; Devault, A.; Arceci, R. J.; Gros, P.; Housman, D. E. *Mol. Cell. Biol.* **1989**, *9*, 1346–1350.
10. Eckford, P. D. W.; Sharom, F. J. *Chem. Rev.* **2009**, *109*, 2989–3011.
11. Baguley, B. C. *Mol. Biotechnol.* **2010**, *46*, 308–316.
12. Szakács, G.; Paterson, J. K.; Ludwig, J. A.; Booth-Genthe, C.; Gottesman, M. M. *Nat. Rev. Drug Discov.* **2006**, *5*, 219–234.
13. Clay, A. T.; Sharom, F. J. *Biochemistry (Mosc.)* **2013**, *52*, 343–354.
14. Jin, M. S.; Oldham, M. L.; Zhang, Q.; Chen, J. *Nature* **2012**, *490*, 566–569.
15. Jabeen, I.; Pleban, K.; Rinner, U.; Chiba, P.; Ecker, G. F. *J. Med. Chem.* **2012**, *55*, 3261–3273.
16. Contino, M.; Zinzi, L.; Cantore, M.; Perrone, M. G.; Leopoldo, M.; Berardi, F.; Perrone, R.; Colabufo, N. A. *Bioorg. Med. Chem. Lett.* **2013**, *23*, 3728–3731.
17. Tardia, P.; Stefanachi, A.; Niso, M.; Stolfa, D. A.; Mangiatordi, G. F.; Alberga, D.;

Nicolotti, O.; Lattanzi, G.; Carotti, A.; Leonetti, F.; Perrone, R.; Berardi, F.; Azzariti, A.; Colabufo, N. A.; Cellamare, S. *J. Med. Chem.* **2014**, *57*, 6403–6418.

18. Pinacho Crisóstomo, F. R.; Carrillo, R.; León, L. G.; Martín, T.; Padrón, J. M.; Martín, V. S. *J. Org. Chem.* **2006**, *71*, 2339–2345.
19. Loddo, R.; Briguglio, I.; Corona, P.; Piras, S.; Loriga, M.; Paglietti, G.; Carta, A.; Sanna, G.; Giliberti, G.; Ibba, C.; Farci, P.; La Colla, P. *Eur. J. Med. Chem.* **2014**, *84*, 8–16.
20. Secci, D.; Carradori, S.; Bizzarri, B.; Bolasco, A.; Ballario, P.; Patramani, Z.; Fragapane, P.; Vernarecci, S.; Canzonetta, C.; Filetici, P. *Bioorg. Med. Chem.* **2014**, *22*, 1680–1689.
21. Hopkins, A. L.; Keserü, G. M.; Leeson, P. D.; Rees, D. C.; Reynolds, C. H. *Nat. Rev. Drug Discov.* **2014**, *13*, 105–121.
22. Palmeira, A.; Sousa, E.; H. Vasconcelos, M.; M. Pinto, M. *Curr. Med. Chem.* **2012**, *19*, 1946–2025.
23. Baumert, C.; Hilgeroth, A. *Anti-Cancer Agents Med. Chem.- Anti-Cancer Agents* **2009**, *9*, 415–436.
24. Karim, M.A.; Linnell, W.H.; Sharp, L.K. *J Pharm pharmacol.* 1960, *12*, 74–81.
25. Lenz, G. R. *J. Org. Chem.*, 1974, *39*, 2846–2851.
26. Pellicani, R. Z.; Stefanachi, A.; Niso, M.; Carotti, A.; Leonetti, F.; Nicolotti, O.; Perrone, R.; Berardi, F.; Cellamare, S.; Colabufo, N. A. *J. Med. Chem.* **2012**, *55*, 424–436.
27. Sahdev et al. *Journal of the Institution of Chemists (India)* 1973, *45*, 221.
28. Skinner, W. A.; Kennedy, J.; Degraw, J.; Johnson H. *J. Med. Chem.* 1969, *12*, 715–717.
29. Colabufo, N. A.; Berardi, F.; Perrone, M. G.; Cantore, M.; Contino, M.; Inglese, C.; Niso, M.; Perrone, R. *ChemMedChem* **2009**, *4*, 188–195.
30. Colabufo, N. A.; Berardi, F.; Cantore, M.; Perrone, M. G.; Contino, M.; Inglese, C.; Niso, M.; Perrone, R.; Azzariti, A.; Simone, G. M.; Paradiso, A. *Bioorg. Med. Chem.* **2008**, *16*, 3732–3743.
31. Sebaugh, J. L. *Pharm Stat.* **2011**, *10*, 128–134.
32. Greco, G.; Novellino, E.; Pellicchia, M.; Silipo, C.; Vittoria, A. *SAR QSAR Environ. Res.* **1993**, *1*, 301–334.
33. Shalaeva, M.; Caron, G.; Abramov, Y. A.; O’Connell, T. N.; Plummer, M. S.; Yalamanchi, G.; Farley, K. A.; Goetz, G. H.; Philippe, L.; Shapiro, M. J. *J. Med. Chem.* **2013**, *56*, 4870–4879.

34. Kitagawa, S. *Biol. Pharm. Bull.* **2006**, *29*, 1–6.
35. Nicolotti, O.; Carotti, A. *J. Chem. Inf. Model.* **2006**, *46*, 264–276.
36. Roy, K.; Paul, S. *QSAR Comb. Sci.* **2009**, *28*, 406–425.
37. Pratim Roy, P.; Paul, S.; Mitra, I.; Roy, K. *Molecules* **2009**, *14*, 1660–1701.
38. Frisch, M. J.; Trucks, G. W.; Schlegel, H. B.; Scuseria, G. E.; Robb, M. A.; Cheeseman, J. R.; Scalmani, G.; Barone, V.; Mennucci, B.; Petersson, G. A.; Nakatsuji, H.; Caricato, M.; Li, X.; Hratchian, H. P.; Izmaylov, A. F.; Bloino, J.; Zheng, G.; Sonnenberg, J. L.; Hada, M.; Ehara, M.; Toyota, K.; Fukuda, R.; Hasegawa, J.; Ishida, M.; Nakajima, T.; Honda, Y.; Kitao, O.; Nakai, H.; Vreven, T.; Montgomery, J. A., Jr.; Peralta, J. E.; Ogliaro, F.; Bearpark, M.; Heyd, J. J.; Brothers, E.; Kudin, K. N.; Staroverov, V. N.; Kobayashi, R.; Normand, J.; Raghavachari, K.; Rendell, A.; Burant, J. C.; Iyengar, S. S.; Tomasi, J.; Cossi, M.; Rega, N.; Millam, J. M.; Klene, M.; Knox, J. E.; Cross, J. B.; Bakken, V.; Adamo, C.; Jaramillo, J.; Gomperts, R.; Stratmann, R. E.; Yazyev, O.; Austin, A. J.; Cammi, R.; Pomelli, C.; Ochterski, J. W.; Martin, R. L.; Morokuma, K.; Zakrzewski, V. G.; Voth, G. A.; Salvador, P.; Dannenberg, J. J.; Dapprich, S.; Daniels, A. D.; Farkas, Ö.; Foresman, J. B.; Ortiz, J. V.; Cioslowski, J.; Fox, D. J. *Gaussian 09*, revision A.2, Gaussian, Inc.: Wallingford, CT, 2009.
39. Becke, A. D. *J. Chem. Phys.* **1993**, *98*, 5648–5652.